Calculation of 3D Eddy Current Fields using both Electric and Magnetic Vector Potential in Conducting Regions

D. Albertz and G. Henneberger
Institut für Elektrische Maschinen, RWTH Aachen, Schinkelstraße 4, 52056 Aachen, Germany

***Abstract*–Most papers concerning the calculation of 3D eddy current problems are using a combination of a vector potential and a scalar potential to solve the electromagnetic field in conducting regions. This paper presents the $\vec{A},\vec{T}$ formulation using both the magnetic vector potential $\vec{A}$ and the electric vector potential $\vec{T}$ for the eddy current regions. Since nodal vector potentials with continuous normal components have accuracy problems at interfaces of regions with different permeabilities, edge elements are used for both potentials. The advantages of the presented formulation compared to the mentioned well-known formulations are described in detail. The formulation is applied on the computation of the 3D time-harmonic eddy current field of an induction furnace and is compared to other formulations as well.**

***Index terms*–Electromagnetic fields, finite element methods, eddy currents, numerical stability, induction heating**

I. Introduction

For the calculation of 3D eddy current fields mostly two different potential formulations have been used. One is the magnetic vector potential $\vec{A}$ and the electric scalar potential V in the $\vec{A},V$ formulation [1], [2], [3], the other is the electric vector potential $\vec{T}$ and the magnetic scalar potential Ω in the $\vec{T}$, Ω formulation [2], [3], [4]. To obtain the uniqueness of the vector potentials in case of the mostly used nodal elements and to gain a better convergence behaviour of the system matrix as well, the Coulomb Gauge is employed leading to a lack of accuracy in the solution [5].

Therefore and because continuous nodal elements leads to numerical problems on interfaces between regions with different permeabilities edge elements are often employed for the vector potentials to obtain a better accuracy of the field solution [6], [7]. But, interpolating the vector potential with edge elements results in a singular system [8], [9].

Since the eddy current density $\vec{J}$ in the $\vec{A},V$ formulation and the flux density $\vec{B}$ in the $\vec{T}$, Ω formulation are only numerically but not exactly divergence free, the singular system matrix may collapse [8]. A tree-cotree gauging [9] is necessary for the matrix to converge, but results in a high number of iteration steps and consequently in an unintentional long computation time. A lot of papers deal with the described disadvantages of the mentioned well-known formulation trying to settle these problems by keeping the given formulations.

Manuscript received November 3, 1997.
G. Henneberger, e-mail henneberger@rwth-aachen.de;
D. Albertz, e-mail albertz@rwth-aachen.de.

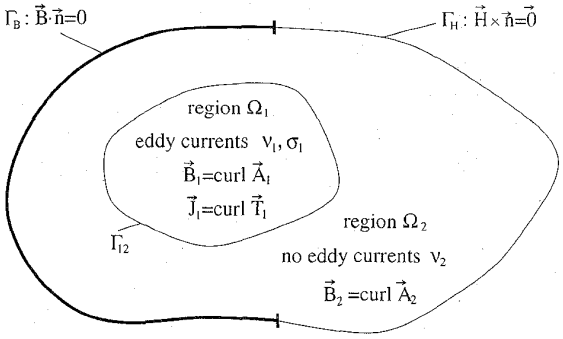

Fig. 1. Typical eddy current field problem

In this paper the problems are eliminated by solving eddy current problems with two vector potentials for both the magnetic and electric field. The inaccuracy of nodal elements is settled by using edge elements. Since the resulting singular system leads to a consistent system with exactly divergence free flux- and current densities a tree-gauge is not necessary and the system shows a very good convergence behaviour.

II. Calculation Methods

A. Problem Definition

Fig. 1 shows a simple configuration of an electromagnetic field problem with one eddy current region. In the eddy current region Ω_1 the following Maxwell equations are valid:

$$\text{curl}\,\vec{H} = \vec{J} \quad (1) \qquad \text{curl}\,\vec{E} = -\frac{\partial \vec{B}}{\partial t} \quad (4)$$

$$\text{div}\,\vec{B} = 0 \quad (2) \qquad \text{div}\,\vec{J} = 0 \quad (5)$$

$$\vec{B} = \mu\vec{H} \quad (3) \qquad \vec{J} = \sigma\vec{E} \quad (6)$$

In the non-conducting part Ω_2, only equations (2) to (4) have to be considered because there are no unknown currents influencing the electromagnetic field problem. In the following only the potential formulation of the conducting region Ω_1 is considered.

B. Common potential formulation

To solve the given Maxwell equations (1) to (6) for the eddy current region Ω_1 mostly one vector potential (3 degrees of freedom (DOF)) and one scalar potential (1 DOF) are combined to a potential formulation. If the magnetic vector potential $\vec{A}$ with $\operatorname{curl}\vec{A} = \vec{B}$ is chosen, the potential equations result in the $\vec{A}, V$ formulation:

$$\operatorname{curl}\nu\operatorname{curl}\vec{A} - \operatorname{grad}\nu\operatorname{div}\vec{A} + \sigma\frac{\partial\vec{A}}{\partial t} + \sigma\operatorname{grad}V = \vec{0} \quad (7)$$

$$\operatorname{div}\left(-\sigma\frac{\partial\vec{A}}{\partial t} - \sigma\operatorname{grad}V\right) = \vec{0} \quad (8)$$

If the electric vector potential $\vec{T}$ with $\operatorname{curl}\vec{T} = \vec{J}$ is chosen, the potential equations result in the $\vec{T}, \Omega$ formulation:

$$\operatorname{curl}\frac{1}{\sigma}\operatorname{curl}\vec{T} - \operatorname{grad}\frac{1}{\sigma}\operatorname{div}\vec{T} + \mu\frac{\partial\vec{T}}{\partial t} - \mu\operatorname{grad}\frac{\partial\Omega}{\partial t} = \vec{0} \quad (9)$$

$$\operatorname{div}\left(\mu\vec{T} - \mu\operatorname{grad}\Omega\right) = \vec{0} \quad (10)$$

Whereas in the $\vec{A}, V$ formulation the magnetic field given by $\vec{B}$ depends only on the derivation of a vector potential, the electric field given by $\vec{J}$ depends on a non-derived vector potential and the gradient of a scalar potential:

$$\vec{B} = \operatorname{curl}\vec{A} \qquad \vec{J} = -\sigma\frac{\partial\vec{A}}{\partial t} - \sigma\operatorname{grad}V \quad (11)$$

In the $\vec{T}, \Omega$ formulation as well the electric field given by $\vec{J}$ depends on the derivation of a vector potential, the magnetic field $\vec{B}$ depends on a non-derived vector potential and the gradient of a scalar potential:

$$\vec{J} = \operatorname{curl}\vec{T} \qquad \vec{B} = \mu\vec{T} - \mu\operatorname{grad}\Omega \quad (12)$$

But this unsymmetrical fact is not necessary to solve the symmetrically looking Maxwell equations (1) - (14) for the conducting regions.

C. The presented $\vec{A}, \vec{T}$ formulation

In this paper a much more symmetric potential formulation for region Ω_1 is presented by using the same potential derivation for the magnetic and the electric field together in one region.

$$\vec{B} = \operatorname{curl}\vec{A} \qquad \vec{J} = \operatorname{curl}\vec{T} \quad (13)$$

This potential set-up results in the presented $\vec{A}, \vec{T}$ formulation, which looks much more symmetric than the common formulations:

$$\operatorname{curl}\nu\operatorname{curl}\vec{A} - \operatorname{curl}\vec{T} = \vec{0} \quad (14)$$

$$\operatorname{curl}\frac{1}{\sigma}\operatorname{curl}\vec{T} + \operatorname{curl}\frac{\partial\vec{A}}{\partial t} = \vec{0} \quad (15)$$

D. Numerical Implementation

Applying the Galerkin weighted residual method to the potential formulations given in (14) and (15) leads to:

$$\int_{\Omega_1}\left(\vec{N}_i\cdot\operatorname{curl}\nu\operatorname{curl}\vec{A} - \vec{N}_i\cdot\operatorname{curl}\vec{T}\right)d\Omega = \vec{0} \quad (16)$$

$$\int_{\Omega_1}\left(\vec{N}_i\cdot\operatorname{curl}\frac{1}{\sigma}\operatorname{curl}\vec{T} + \vec{N}_i\cdot\operatorname{curl}\frac{\partial\vec{A}}{\partial t}\right)d\Omega = \vec{0} \quad (17)$$

Using vector identities and Gauss' theorem as well as defining the $\vec{T} = -\frac{\partial\vec{T}}{\partial t}$ as the negative time derivative of $\vec{T}$, equation (16) and (17) result in a symmetric equation system:

$$\int_{\Omega_1}\left(\nu\operatorname{curl}\vec{N}_i\cdot\operatorname{curl}\vec{A} + \vec{N}_i\cdot\operatorname{curl}\frac{\partial\vec{T}}{\partial t}\right)d\Omega = \vec{0} \quad (18)$$

$$\int_{\Omega_1}\left(-\frac{1}{\sigma}\operatorname{curl}\vec{N}_i\cdot\operatorname{curl}\frac{\partial\vec{T}}{\partial t} + \operatorname{curl}\vec{N}_i\cdot\frac{\partial\vec{A}}{\partial t}\right)d\Omega = \vec{0} \quad (19)$$

In principle this formulation can be applied as well on nodal as on edge elements and for any kind of geometry (hexahedrons, bricks, pyramids).

Because of the numerical inaccuracy of nodal elements and to save the disadvantage of 6 DOF for each node, in this paper linear edge based tetrahedral elements are used, which 2 DOF for $\vec{A}$ and $\vec{T}$ on each edge. With the presented formulation all types of eddy current regions (current driven coils, open or short conductors) can be considered.

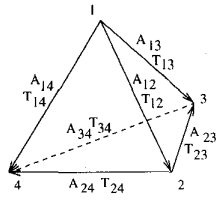

$$\vec{A}(x,y,z) = \sum_{i=1}^{3}\sum_{j=i+1}^{4}\vec{\alpha}_{ij}A_{ij} \quad (20)$$

$$\vec{T}(x,y,z) = \sum_{i=1}^{3}\sum_{j=i+1}^{4}\vec{\alpha}_{ij}T_{ij} \quad (21)$$

$$\text{with}\quad \vec{\alpha}_{ij} = N_i\nabla N_j - N_j\nabla N_i \quad (22)$$

III. Application

A. Comparison of the potential formulations

Fig. 2 displays a simple test model for the comparison between the well-known $\vec{A} - \vec{A}, V$ potential formulation with nodal elements and the presented edge based $\vec{A} - \vec{A}, \vec{T}$ formulation. It consists of three conducting regions of copper ($\sigma = 5.7 \cdot 10^7\ \mathrm{Sm}^{-1}$) between two iron yokes ($\mu_r = 1000$, $V = 100 \cdot 55 \cdot 100\ \mathrm{mm}^3$) in a homogeneous magnetic field of 50 mT (4000 Hz) in y-direction.

Because of the symmetry only one quarter of the model has to be calculated. The first conductor in the middle ($d = 10$ mm) is considered to be short, the second conductor ($d = 10$ mm, $r = 20$ mm) is an open coil and the third one ($d = 10$ mm, $r = 40$ mm) represents a current driven coil ($I = 40$ A). The mesh consists of 1st order tetrahedral elements.

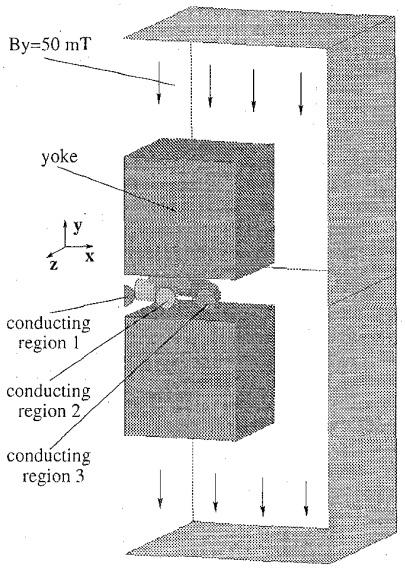

Fig. 2. Test model

Table I compares the two computation methods concerning some mesh and solving data. In the presented edge based formulation the number of DOF is more than 2.6 times higher than in the nodal based $\vec{A}-\vec{A},V$ formulation. A factor of 2 results by the fact that there are more than 6 times more edges than nodes in a tetrahedral mesh, but there are 3 DOF per node instead of one per edge for the vector potential $\vec{A}$. The reason for the rest of the factor 2.6 is, that there are more unknowns in the conducting region taking the edge based electric vector potentials $\vec{T}$ instead of the nodal based electric scalar potential V.

But in the case of edge elements the matrix is much sparser ($48 < 94$, $0.112\% < 0.568\%$), so that the number of non zeros has only a factor of 1.3 between the 2 formulations. The sparseness of the matrix is one of the reason, why the edge based $\vec{A}-\vec{A},\vec{T}$ formulation has a similar good convergence behaviour (81 compared to 78 ICCG steps) like the $\vec{A}-\vec{A},V$ formulation with implemented Coulomb gauge.

TABLE I
Comparison between the two formulations

Formulation	$\vec{A}-\vec{A},\vec{T}$	$\vec{A}-\vec{A},V$
Nodes	4820	4820
Elements	24902	24902
Edges	30701	30701
Order	1	1
number of DOF	43047	16565
Non zeros	2083246	1557490
Matrix density	0.112 %	0.568 %
Average columns per line	48	94
Solver	ICCG	ICCG
number of ICCG steps	81	78
CPU time (HP J280)	399 s	297 s
Power loss conductor 1	14.4 W	10.4 W
Power loss conductor 2	212 W	232 W
Power loss conductor 3	333 W	399 W
Accuracy	+	−

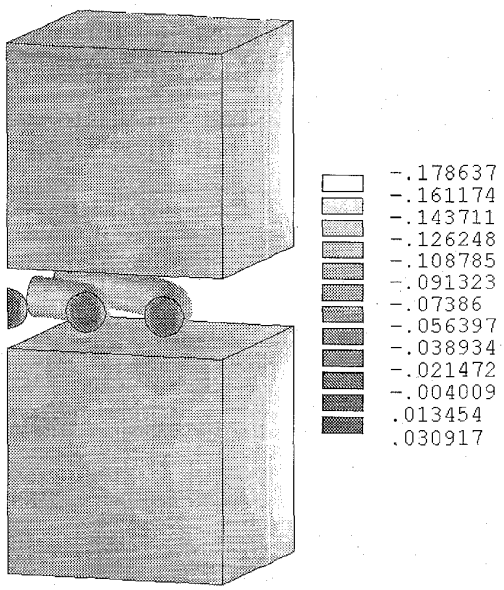

Fig. 3. Flux density $\vec{B}$ (T) in y direction ($\vec{A}-\vec{A},\vec{T}$ formulation)

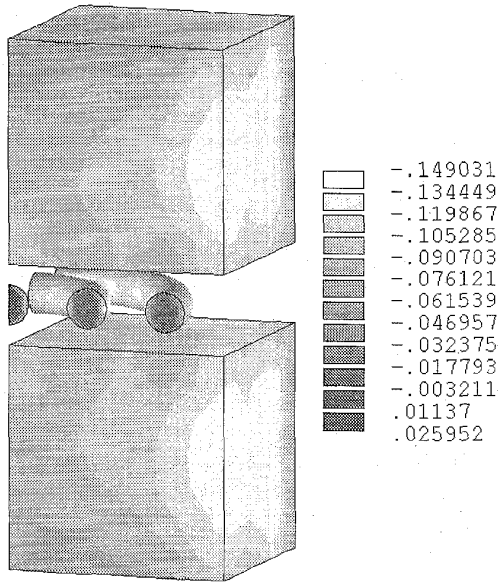

Fig. 4. Flux density $\vec{B}$ (T) in y direction ($\vec{A}-\vec{A},V$ formulation)

However, the main advantage of the presented formulations is the accuracy of edge elements which produces a much better result on iron-air interfaces than nodal elements without free normal components do. Fig. 3 and 4 show the differences in the y-component of the real part of the flux density $\vec{B}$ on the iron interfaces. Fig. 4 belonging to the nodal $\vec{A}-\vec{A},V$ formulation with Coulomb gauge shows a wrong field solution on the iron interfaces, which also leads to mistakes in the complete distribution

and in the loss power of the three conduction regions (see Table I).

The other advantage is that the presented formulation results in a consistent matrix system, so that a tree-cotree gauge is not necessary and the matrix demonstrates a very good convergence behaviour.

B. Computation the power losses of an induction furnace

Finally the presented formulation is applied to the calculation of the electromagnetic eddy current field of an induction furnace shown in Fig. 5. A water cooled copper coil causes a time harmonic field of 500 Hz which leads to high eddy currents in the melt. The surrounding yokes insure, that the magnetic flux is directed close to the coil, and reduce the magnetic flux leakage.

It is important that the power efficiency of the furnace is very high. So the loss power of each turn of the coil displayed in fig. 6 is of high interest.

Fig. 6 states, that the 3D calculation gives similar results compared to the axially symmetrical 2D calculation, which shows that the accuracy of the 3D presented $\vec{A},\vec{T}$ formulation is just as good as we know it from 2D calculation and that the influence of the non axially symmetrical yoke can be nearly neglected.

IV. Conclusion

In this paper the $\vec{A}$, $\vec{T}$ formulation for 3D eddy current problems based on edge elements is presented. The results agree well to other computation methods. The advantages of the presented formulation to other well-known potential formulations are detailed described. Finally the formulation is compared to other formulations and applied to the calculation of an induction furnace.

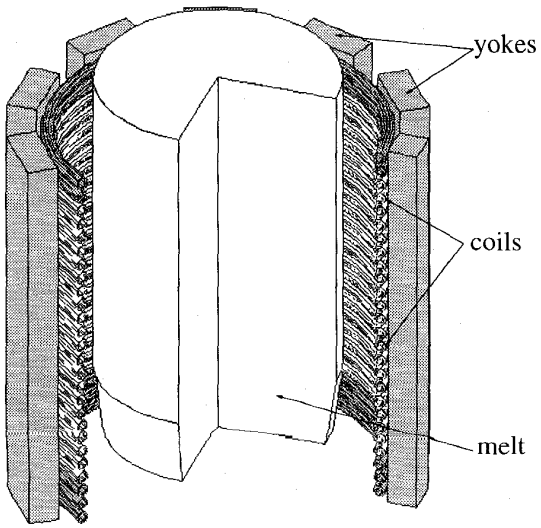

Fig. 5. Structure of an induction furnace

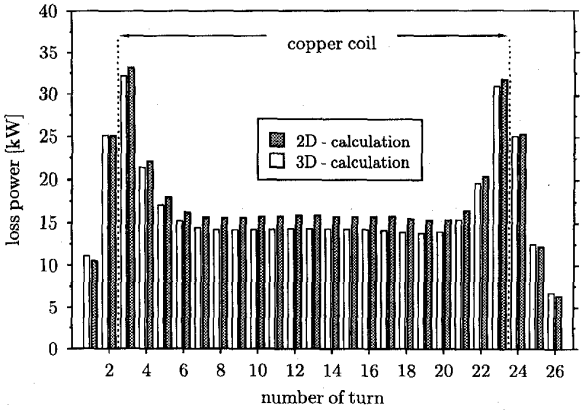

Fig. 6. Loss power of each turn

References

[1] O. Biro, K. Preis, "On the use of magnetic vector potential in the finite element analysis of three-dimensional eddy currents", *IEEE Trans. Magn.*, vol. 25, no 4, pp. 3145-3159, July 1989.

[2] O. Biro, K. Preis, "Finite element analysis of 3-D eddy currents", *IEEE Trans. Magn.*, vol. 26, no 2, pp. 418-423, March 1990.

[3] W. Renhart, H. Stögner, K. Preis, "Calculation of 3D eddy current problems by finite element method using either an electric or a magnetic vector potential", *IEEE Trans. Magn.*, vol. 24, no 1, pp. 122-125, January 1988.

[4] R. Albanese, G. Rubinacci, "Solution of three dimensional eddy current problems by integral and differential methods", *IEEE Trans. Magn.*, vol. 24, no 1, pp. 98-101, January 1988.

[5] D. Albertz, S. Dappen, G. Henneberger, "Calculation of the induced currents and forces for a hybrid magnetic levitation system", *IEEE Trans. Magn.*, vol. 32, no 3, pp. 1263-1266, May 1996.

[6] G. Mur, "Edge Elements, their advantages and their disadvantages ", *IEEE Trans. Magn.*, vol. 30, no 5, pp. 3552-3557, September 1994.

[7] A. Bossavit, "A rationale for edge elements", *IEEE Trans. Magn.*, vol. 24, no 1, pp. 74-79, January 1988.

[8] O. Biro, K. Preis, K. R. Richter, "On the use of magnetic vector potential in the nodal and edge finite element analysis of 3D magnetostatic fields", *IEEE Trans. Magn.*, vol. 32, no 3, pp. 651-654, May 1996.

[9] J. B. Manges, Z. J. Cendes, "a generalized tree-cotree gauge for magnetic field computation", *IEEE Trans. Magn.*, vol. 31, no 3, pp. 1342-1347, May 1995.